Int. J. Electrochem. Sci., 17 **(2022)** Article Number: 220516, doi: 10.20964/2022.04.58

International Journal of
ELECTROCHEMICAL
SCIENCE
www.electrochemsci.org

Short Communication

Electrochemical and Theoretical Study of Corrosion Inhibition on X60 Steel in H_2SO_4 Solution by Omeprazole

Yanxia Liu[1], *Wei Du*[2], *Xiuquan Yao*[3,*], *Chunlin Liu*[4], *Xiaofang Luo*[5], *Lei Guo*[6,*], *Chao Guo*[7]

[1] College of Chemistry and Chemical Engineering, Jining Normal University, Ulanqab 012000, China.
[2] Metals and Chemistry Research Institute, China Academy of Railway Sciences Corporation Limited, Beijing, 100081, China.
[3] National Center for Materials Service Safety, University of Science and Technology Beijing, Beijing, 100083, China.
[4] Latin America Branch, China Petroleum Engineering & Construction Corporation (CPECC), Beijing, 100120, China
[5] China Chongqing Academy of Metrology and Quality Inspection, Chongqing, 402160, China.
[6] School of Material and Chemical Engineering, Tongren University, Tongren, 554300, China.
[7] Compact Strip Plant, BaoTou Iron and Steel Co., Ltd., Baotou Inner Mongolia, 014010, China.
[*]E-mail: b20180439@xs.ustb.edu.cn (X. Yao), chygl@gztrc.edu.cn (L. Guo).

Received: 11 December 2021 / *Accepted:* 13 February 2022 / *Published:* 5 April 2022

The corrosion inhibition performance of Omeprazole (OMP) on X60 steel in 0.5M H_2SO_4 solution was studied by electrochemical impedance spectroscopy and electrochemical polarization curves. These tests are complemented by theoretical calculations using molecular dynamics. The corrosion inhibition efficiency increases with the concentration of OMP, a hybrid corrosion inhibitor that adsorbs on X60 steel following the Langmuir adsorption isotherm. The adsorption configuration calculated by molecular dynamics showed that the OMP molecules were arranged in parallel on the surface of X60 steel, which ensured its excellent inhibition performance.

Keywords: Mild steel; Corrosion inhibitor; Sulfuric acid solution; EIS; SEM

1. INTRODUCTION

With the development of society and the improvement of living standards, a large number of infrastructures are being built and the demand for steel is growing. With its low price and reliable performance, steel has become one of the most used materials in the world and is the material foundation of modern society. Steel consumption in the rapid growth at the same time, there are many problems, such as: steel structures in the environment is easy to rust and corrosion, poor corrosion resistance, and

corrosion is a very widespread problem, China's annual economic losses caused by corrosion, accounting for about 3% of the gross national product [1]. Corrosion has become a common concern for steel materials.

At present, researchers in various countries for the means of corrosion prevention from macroscopic to microscopic conducted many studies. For corrosion prevention problems are often used to change the nature of the metal, corrosion inhibitor method, electrochemical protection method and other means [2-10]. Corrosion inhibitor method is the most convenient to use, the simplest process and the most cost-effective method, is now widely used in chemical cleaning, rust prevention between processes, metal products storage and transportation, cooling water treatment and oil extraction and other projects [11-15]. Zuo et al [16] studied the corrosion protection effect of a plant green corrosion inhibitors on X70 steel using theoretical calculations, weight loss and electrochemical methods. Two food flavorants as new corrosion inhibitors of mild steel in H_2SO_4 solution was studied by Tan et al [17] from a microscopic point of view using electrochemical impedance spectroscopy and electrochemical polarization techniques.

In recent years, drug molecules have been frequently used as corrosion retardants [18-29]. Omeprazole (OMP) molecule contains several N, O, S atoms, so this experiment investigated its protective effect on X60 steel in sulfuric acid solution. Electrochemical experiments were used to evaluate the anti-corrosion efficiency of the OMP molecule and to explain theoretically why OMP can be used as a corrosion inhibitor.

2. EXPERIMENTAL

2.1 Chemicals

The steel used for all experiments was X60, and the corrosion inhibitor OMP was purchased from Aladdin, analytical and pharmaceutical with a purity greater than 98%. Fig. 1 shows its molecular structure. The X60 specimens used for electrochemical experiments were epoxy-coated, allowing an exposed area of 1 cm^2. Before each experiment, the samples were ground and polished with SiC sandpaper (from 600 to 2000) and cleaned with deionized water. Dilute concentrated sulfuric acid to 0.5 M as the corrosive medium in this experiment. Adding different quality of OMP corrosion inhibitor (100, 200, 300 mg) to 1 L sulfuric acid solution was also used as corrosion medium.

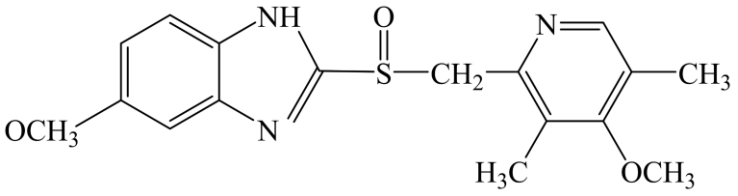

Figure 1. Chemical structure of Omeprazole

2.2 Electrochemical experiment

All electrochemical measurements were performed on a Gamry 600+ instrument, and electrochemical impedance spectroscopy (EIS) was used to fit curves and analyze relevant parameters with Zsimpwin software. The electrochemical properties of X60 samples in uninhibited and inhibited solutions were achieved in a conventional three-electrode cell: X60 as working electrode, platinum electrode as counter electrode, and saturated calomel electrode (SCE) as reference. Electrochemical impedance spectroscopy (EIS) experiments were carried out in the frequency range from 100 kHz to 10 mHz. When the X60 sample was soaked in sulfuric acid solution for 30 min, the signal amplitude disturbance relative to the open circuit potential (OCP) of 10 mV was measured. Potential dynamic polarization curves of X60 in sulfuric acid solution were recorded from －250 mV to 250 mV (Vs OCP), at a scan rate of 1 mV/s.

2.3 Surface Analysis

The morphology of X60 surface after immersion in 0.5 M sulfuric acid solution without and with addition of 300 mg/L OMP for 4 h at 298K was measured by scanning electron microscope.

2.4 MD calculation

The adsorption model of OMP molecule and X60 was simulated by molecular dynamics simulation method. Under the action of the COMPASS force field, the simulation is performed in a box with controlled periodic boundary conditions of (24.2*17.0*71.8) Å, and each layer containing one DPD molecule and 200 water molecules. Meanwhile, the Fe (110) crystal plane was selected as a representative. The simulation conditions were NVT ensemble, and the time step was 300 ps. The adsorption model and adsorption energy of the corrosion inhibitor on the X60 surface were obtained and analyzed.

3. RESULTS AND DISCUSSION

3.1 Electrochemical testing

Fig. 2 shows the OCP curves of X60 in 0.5M H_2SO_4 with different concentrations of OMP inhibitor at 298K. As shown in the figure, at each concentration, the value of OCP will fluctuate for a period of time, and finally tend to be stable. This behavioral change may be due to the stable adsorption of OMP molecules on the surface of the X60 sample. With the increase of OMP concentration, the value of OCP moves to the positive direction.

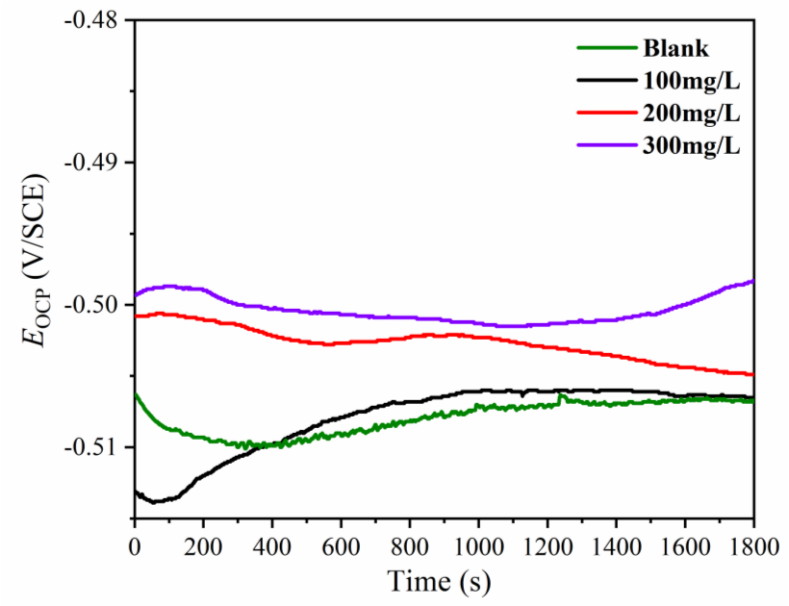

Figure 2. OCP curves for X60 in 0.5 M H_2SO_4 without and with OMP at 298K

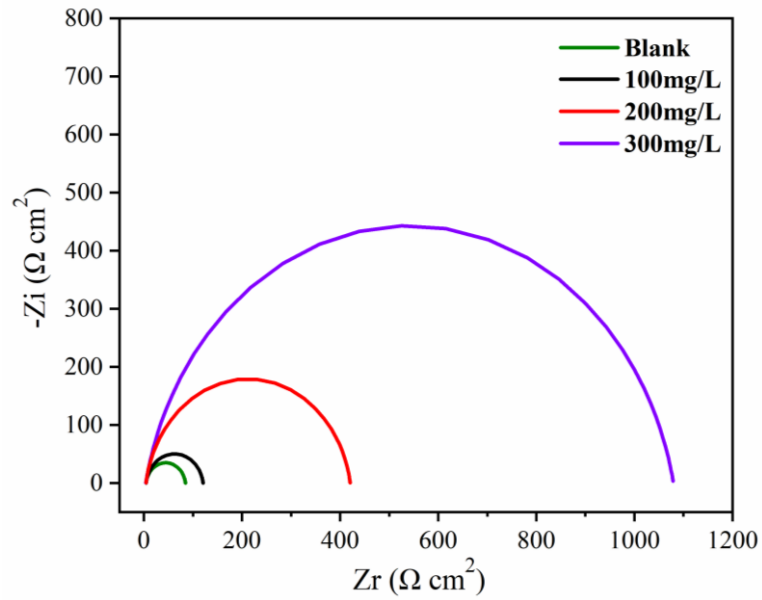

Figure 3. Nyquist plots for X60 in 0.5 M H_2SO_4 without and with OMP at 298K

Electrochemical impedance spectroscopy (EIS) can provide very useful information in inferring the corrosion inhibition mechanism. The EIS-based corrosion inhibitor performance can be expressed by Eq. (1)

$$\eta\ (\%) = (R_{ct} - R_{ct}^{0})/R_{ct} \times 100\% \quad (1)$$

where R_{ct} and R_{ct}^{0} are the transfer resistances in the presence and absence of OMP, respectively.

Fig. 3 shows the Nyquist plots of X60 steel in sulfuric acid solutions with different concentrations of OMP added. The Nyquist plot contains only one semicircle with a diameter reflecting the R_{ct} value [30-32].

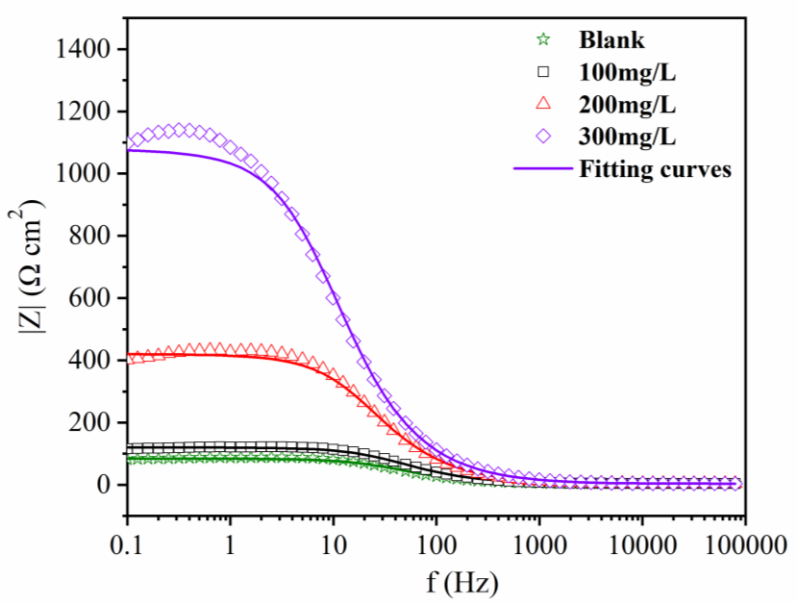

Figure 4. Bode plots for X60 in 0.5 M H_2SO_4 without and with OMP at 298K

The increasing diameters of Nyquist plots for different OMP additions indicate that the corrosion inhibition potential in 0.5 M H_2SO_4 solution increases with the amount of corrosion inhibitor added. The shape of the capacitor ring in the figure is a concave semicircle. This may be due to the electrode dispersion effect due to the uneven electrode surface [33-35]. The performance of double-layer capacitors is different from that of ideal capacitors, so it is necessary to select an appropriate circuit fit for the impedance spectrum [36-38]. In this study, the equivalent circuit used to fit the experimental results is shown in Fig. 5. The EIS parameters obtained after the proposed circuit fitting are shown in Table 1.

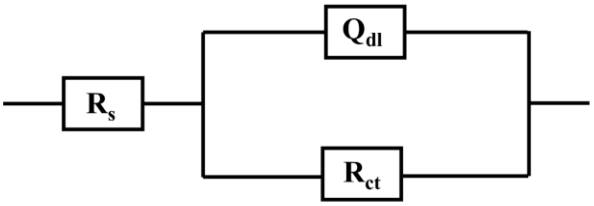

Figure 5. Equivalent circuit model of the X60 electrodes in 0.5 M H_2SO_4 solution

In the circuit, R_s presents the solution resistance, R_{ct} is the charge transfer resistance, and constant phase element (CPE) is used instead of capacitive components. The impedance of CPE is described as follows [39, 40]:

$$Z_{cpe}=1/(Y_0(j\omega)^n) \quad (2)$$

where j: the imaginary root, ω: the angular frequency, Y_0: proportional factor, and n: the CPE index associated with the inherent chemical and physical heterogeneous characters of the solid surfaces. The CPE can show a resistor (n = 0), a Warburg impedance (n = 0.5), or a capacitor (n = 1).

Table 1. Electrochemical impedance parameters obtained for X60 in 0.5 M H_2SO_4 without and with OMP at 298K

C (mg/L)	R_s (Ω cm^2)	R_{ct} (Ω cm^2)	CPE ($10^{-5}\Omega^{-1}s^n cm^{-2}$)	n	η (%)
0	4.1	80.4	9.9	0.91	
100	4.3	156.2	6.6	0.91	48.51
200	4.1	416.4	3.5	0.90	80.68
300	3.7	1076	3.1	0.88	92.52

It is obvious from Table 1 that the corrosion of X60 in sulfuric acid solution is inhibited with the addition of OMP. With the increase of OMP concentration in sulfuric acid solution, the value of CPE gradually decreased and the value of R_{ct} gradually increased. When 300 mg/L of OMP was added, the best inhibition efficiency was achieved, which was 92.52%. The results show that OMP molecules are adsorbed on the surface of the X60 electrode, protecting it from corrosion.

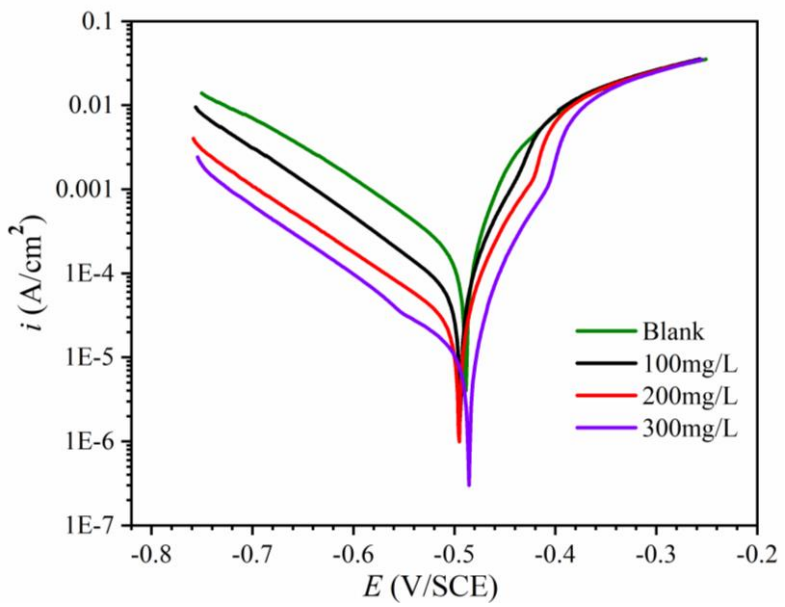

Figure 6. Potentiodynamic polarization curves for X60 in 0.5 M H_2SO_4 solution without and with OMP at 298K

Usually Tafel polarization can obtain some information about the electrode reaction mechanism and inhibitor effect. The polarization method enables the experimental measurement of the instantaneous reaction rate at the metal-solution interface. Fig. 6 shows the potentiodynamic polarization curves for X60 in the absence and presence of various concentrations of OMP corrosion inhibitor in 0.5 M H_2SO_4 solution. The polarization curve was analyzed, the corresponding parameters (corrosion potential (E_{corr}), corrosion current density (i_{corr}), anodic (β_a), cathodic (β_c) Tafel slopes) were obtained, and the inhibition efficiency was calculated (Table 2).

$$\eta\ (\%) = (i_{corr,0} - i_{corr})/(i_{corr,0}) \times 100\% \quad (3)$$

Where, $i_{corr,0}$ and i_{corr} stands for the value of corrosion current density for the bare acid solution and inhibited acid solution, respectively.

Table 2. The polarization parameters obtained for X60 in 0.5 M H_2SO_4 without and with OMP at 298K

C (mg/L)	E_{corr} (mV/SCE)	i_{corr} (μA cm^{-2})	β_a (mV dec^{-1})	β_c (mV dec^{-1})	η (%)
0	−489	125.70	35	−79	
100	−499	55.78	41	−99	55.62
200	−495	27.87	38	−121	77.83
300	−486	13.06	37	−119	89.61

With the gradual increase of the amount of OMP corrosion inhibitor, the corrosion current density continued to decrease. The cathodic polarization curves are almost parallel, indicating that the cathodic reaction mechanism is consistent [41, 42]. OMP inhibitors reduce the corrosion rate by covering the active sites present on the electrode surface. In addition, compared with the blank acid solution, the corrosion potential (E_{corr}) after adding the inhibitor did not change significantly ($<$ 85 mV), indicating that the OMP inhibitor is a mixed inhibitor, which controls the corrosion reaction of the anode and the cathode [38, 43]. The corrosion rate is the smallest when 300 mg/L was added to the sulfuric acid solution, and the sustained release efficiency can reach 89.61%.

3.2 SEM analysis

In order to validate the protective effect of OMP corrosion inhibitor on X60 steel, the surface morphology of steel immersed in sulfuric acid solution with and without OMP inhibitor for 4 hours was observed, as shown in Fig. 7. Fig. 7a shows the surface morphology of the sample without corrosion inhibitor. X60 steel was seriously corroded, and the surface was irregular and rough. After adding 300 mg/L OMP (Fig. 7b), the surface of X60 was well protected, and the mechanical polishing scratches could be clearly seen, but the pits also existed. The comparison between the two samples shows that OMP has a strong protective effect on X60 steel, which is due to the formation of a protective film on the surface of the sample.

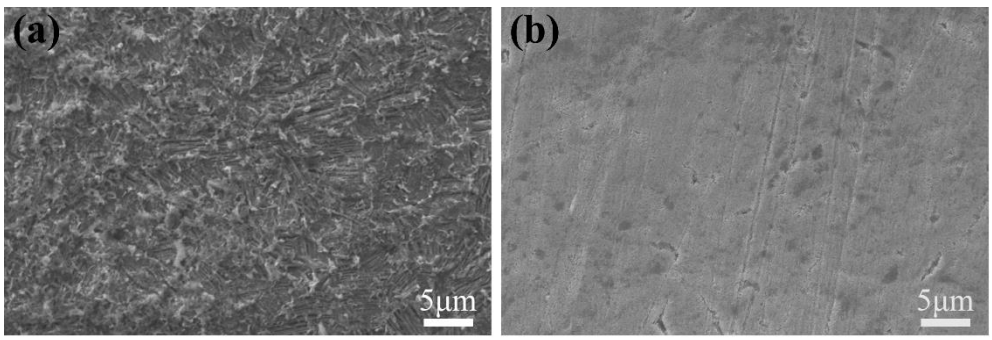

Figure 7. SEM images of bare X60 (a) and with 300 mg/L OMP (b) after being immersed in 0.5 M H_2SO_4 solution for 4 h

3.3 Adsorption isotherm

The compactness and adhesion of the protective layer on the metal surface are mainly determined by the structure of the corrosion inhibitor. Therefore, the adsorption of OMP molecules on the surface of X60 steel was also investigated. The adsorption process is usually described by adsorption isotherms. Use equation (4) to obtain the correct isotherm [44].

$$C/\theta = 1/K_{ads} + C \quad (4)$$

where C is the concentration of the inhibitor, K_{ads} represents the adsorption equilibrium constant, and θ (surface coverage) is defined as the corrosion inhibition efficiency obtained from the polarization curve measurements.

The fitted line plot for C/θ in function of C (Fig. 8) follows the Langmuir adsorption model, and the regression coefficient (R^2) is close to 1. The free energy of adsorption ΔG^0_{ads} was calculated as follows:

$$K_{ads} = 1/C_s \, exp(\frac{-\Delta G^0_{ads}}{RT}) \quad (5)$$

Herein, R is the molar gas constant (8.314 J mol $^{-1}$ K $^{-1}$) and T is the absolute temperature (K), C_s corresponds to the concentration of water in solution (1×10^3 g/L). The calculated Gibbs free energy is about −26.06 kJ mol^{-1}. In general, ΔG^0_{ads} values indicating physical adsorption are around −20 kJ mol^{-1} or more positive, while values around −40 kJ mol^{-1} or more negative favor chemisorption. Therefore, the adsorption of OMP on the surface of X60 has both physical and chemical adsorption[45, 46].

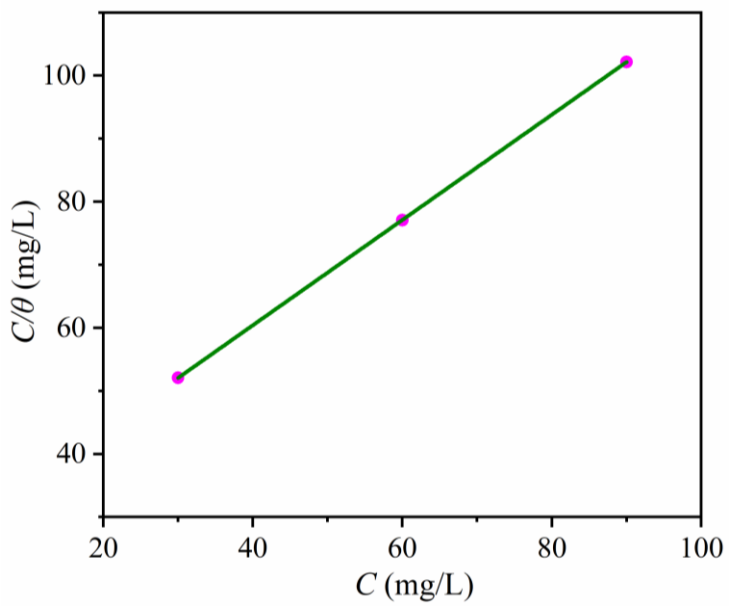

Figure 8. Langmuir adsorption plots of OMP on the X60 electrodes in 0.5 M H_2SO_4 solution

3.4 Molecular dynamics calculation

To theoretically explain the excellent inhibition effect of OMP, the adsorption configuration of OMP on Fe (110) was calculated by molecular dynamics. Fig. 9 shows the equilibrium adsorption configuration of OMP corrosion inhibitor on Fe (110) matrix, including top view. As shown in the figure, the OMP molecules are adsorbed on the steel surface in a planar form, which ensures the maximum coverage and thus can effectively hinder the attack of corrosive ions. In addition, the adsorption energy of OMP was calculated to be −289.2 kJ mol^{-1}, and a larger adsorption energy is also beneficial to the formation of a dense protective film on the steel surface [47-49].

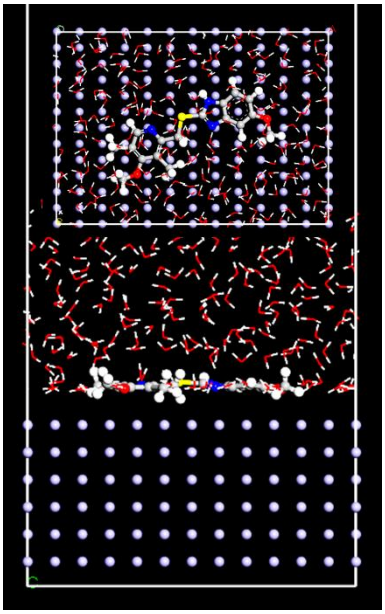

Figure 9. Equilibrium adsorption configuration of OMP corrosion inhibitor on Fe (110) substrate (inset: on-top view)

4. CONCLUSION

Summarizing the work of this study, a drug molecule, OMP, was evaluated as a corrosion inhibitor for X60 steel in sulfuric acid solution, and the following conclusions were drawn from the study: The EIS and PD results fully demonstrated that OMP in sulfuric acid solution can protect X60 steel well, and the inhibition efficiency is proportional to the additive concentration, and the efficiency can reach 92.52% when the additive content is 300 mg/L. The surface morphology of the soaked X60 steel well verified the results of the electrochemical experiments. The adsorption of corrosion inhibitors on carbon steel surfaces follows the Langmuir isotherm. Furthermore, it is theoretically demonstrated that the excellent corrosion resistance of OMP is due to its horizontal configuration on the steel surface.

ACKNOWLEDGMENTS
This work was partly sponsored by the Foundation of the Department of Science and Technology of Guizhou province (QKHPTRC[2021]5643).

References

1. B. Hou, X. Li, X. Ma, C. Du, D. Zhang, M. Zheng, W. Xu, D. Lu, F. Ma, *NPJ. Mater. Degrad.*, 1 (2017).
2. Y. Qiang, H. Zhi, L. Guo, A. Fu, T. Xiang, Y. Jin, *J. Mol. Liq.*, 351 (2022) 118638.
3. M. Ramezanzadeh, G. Bahlakeh, B. Ramezanzadeh, *J. Mol. Liq.*, 292 (2019).
4. Y. Qiang, S. Zhang, S. Xu, W. Li, *J. Colloid. Interf. Sci.*, 472 (2016) 52-59.
5. T. Ge, W. Zhao, X. Wu, X. Lan, Y. Zhang, Y. Qiang, Y. He, *J. Colloid. Interf. Sci.*, 567 (2020) 113-125.
6. M. Huang, G. Lu, J. Pu, Y. Qiang, *J. Ind. Eng. Chem.*, 103 (2021) 154-164.
7. H. Li, Y. Qiang, W. Zhao, S. Zhang, *Corros. Sci.*, 191 (2021) 109715.
8. L. Ma, Y. Qiang, W. Zhao, *Chem. Eng. J.*, 408 (2021) 127367.
9. M. Ramezanzadeh, G. Bahlakeh, B. Ramezanzadeh, *J. Mol. Liq.*, 290 (2019) 111212.
10. Y. Qiang, S. Fu, S. Zhang, S. Chen, X. Zou, *Corros. Sci.*, 140 (2018) 111-121.
11. P. Han, C. Chen, W. Li, H. Yu, Y. Xu, L. Ma, Y. Zheng, *J. Colloid. Interf. Sci.*, 516 (2018) 398-406.
12. X. He, J. Mao, Q. Ma, Y. Tang, *J. Mol. Liq.*, 269 (2018) 260-268.
13. P. Kannan, T.S. Rao, N. Rajendran, *J. Colloid. Interf. Sci.*, 512 (2018) 618-628.
14. Marija B. Petrović, Milan B. Radovanović, Ana T. Simonović, Snežana M. Milić, Milan M. Antonijević, *Int. J. Electrochem. Sci.*, 7 (2012) 9043-9057.
15. Marija B. Petrović Mihajlović, Milan M. Antonijević, *Int. J. Electrochem. Sci.*, 10 (2015) 1027-1053.
16. X. Zuo, W. Li, W. Luo, X. Zhang, Y. Qiang, J. Zhang, H. Li, B. Tan, *J. Mol. Liq.*, 321 (2021) 114914.
17. B. Tan, S. Zhang, H. Liu, Y. Guo, Y. Qiang, W. Li, L. Guo, C. Xu, S. Chen, *J. Colloid. Interf. Sci.*, 538 (2019) 519-529.
18. M. Abdallah, *Corros. Sci.*, 46 (2004) 1981-1996.
19. M.M. El-Naggar, *Corros. Sci.*, 49 (2007) 2226-2236.
20. I.B. Obot, N.O. Obi-Egbedi, S.A. Umoren, *Corros. Sci.*, 51 (2009) 1868-1875.
21. S.K. Shukla, M.A. Quraishi, *Corros. Sci.*, 51 (2009) 1007-1011.
22. I. Ahamad, R. Prasad, M.A. Quraishi, *Corros. Sci.*, 52 (2010) 3033-3041.
23. I. Ahamad, M.A. Quraishi, *Corros. Sci.*, 52 (2010) 651-656.
24. S.M. Azab, A.M. Fekry, *J. Alloy. Compd.*, 717 (2017) 25-30.
25. Ž.Z. Tasić, M.B. Petrović Mihajlović, M.B. Radovanović, M.M. Antonijević, *J. Mol. Liq.*, 265 (2018) 687-692.
26. R.A. Anaee, I.H.R. Tomi, M.H. Abdulmajeed, S.A. Naser, M.M. Kathem, *J. Mol. Liq.*, 279 (2019) 594-602.
27. B. Tan, S. Zhang, Y. Qiang, L. Feng, C. Liao, Y. Xu, S. Chen, *J. Mol. Liq.*, 248 (2017) 902-910.
28. H. Li, S. Zhang, B. Tan, Y. Qiang, W. Li, S. Chen, L. Guo, *J. Mol. Liq.*, 305 (2020) 112789.
29. Y. Qiang, L. Guo, H. Li, X. Lan, *Chem. Eng. J.*, 406 (2021) 126863.
30. Q. Deng, H.-W. Shi, N.-N. Ding, B.-Q. Chen, X.-P. He, G. Liu, Y. Tang, Y.-T. Long, G.-R. Chen, *Corros. Sci.*, 57 (2012) 220-227.
31. S. Tu, X. Jiang, L. Zhou, M. duan, H. Wang, X. Jiang, *Corros. Sci.*, 65 (2012) 13-25.
32. A.O. Yüce, G. Kardaş, *Corros. Sci.*, 58 (2012) 86-94.
33. Y. Qiang, S. Zhang, L. Guo, X. Zheng, B. Xiang, S. Chen, *Corros. Sci.*, 119 (2017) 68-78.

34. Y. Qiang, S. Zhang, S. Yan, X. Zou, S. Chen, *Corros. Sci.*, 126 (2017) 295-304.
35. G. Xia, X. Jiang, L. Zhou, Y. Liao, M. Duan, H. Wang, Q. Pu, J. Zhou, *J. Ind. Eng. Chem.*, 27 (2015) 133-148.
36. R. Yıldız, *Corros. Sci.*, 90 (2015) 544-553.
37. Y. Qiang, S. Zhang, B. Tan, S. Chen, *Corros. Sci.*, 133 (2018) 6-16.
38. M. Prabakaran, S.-H. Kim, N. Mugila, V. Hemapriya, K. Parameswari, S. Chitra, I.-M. Chung, *J. Ind. Eng. Chem.*, 52 (2017) 235-242.
39. P.E. Alvarez, M.V. Fiori-Bimbi, A. Neske, S.A. Brandán, C.A. Gervasi, *J. Ind. Eng. Chem.*, 58 (2018) 92-99.
40. X. Ma, X. Jiang, S. Xia, M. Shan, X. Li, L. Yu, Q. Tang, *Appl. Surf. Sci.*, 371 (2016) 248-257.
41. G. Sığırcık, T. Tüken, M. Erbil, *Corros. Sci.*, 102 (2016) 437-445.
42. Y. Qiang, S. Zhang, H. Zhao, B. Tan, L. Wang, *Corros. Sci.*, 161 (2019) 108193.
43. P. Dohare, K.R. Ansari, M.A. Quraishi, I.B. Obot, *J. Ind. Eng. Chem.*, 52 (2017) 197-210.
44. J. Haque, K.R. Ansari, V. Srivastava, M.A. Quraishi, I.B. Obot, *J. Ind. Eng. Chem.*, 49 (2017) 176-188.
45. K. Hu, J. Zhuang, J. Ding, Z. Ma, F. Wang, X. Zeng, *Corros. Sci.*, 125 (2017) 68-76.
46. Y. Qiang, S. Zhang, L. Wang, *Appl. Surf. Sci.*, 492 (2019) 228-238.
47. Y. Qiang, H. Li, X. Lan, *J. Mater. Sci. Technol.*, 52 (2020) 63-71.
48. L. Guo, S. Kaya, I.B. Obot, X. Zheng, Y. Qiang, *J. Colloid. Interf. Sci.*, 506 (2017) 478-485.